# MODELING AND COMPUTATIONAL SIMULATION OF PHOTOCATALYSIS OF A BISMUTH OXYALURER FOR AIR REMEDIATION

**Solares E., Morales M.A., Luna-Flores A., Cervantes-Tavera A.M., Hernández-Santiago A.A.**
Meritorious Autonomous University of Puebla
*Puebla, Mexico*
Received: 20.07.2020

**Introduction.**

Bismuth-based materials have been extensively studied due to their possible applications in various areas, especially used as promising photocatalysts for the removal of persistent organic pollutants (COP). Advanced oxidation processes that employ highly oxidizing hydroxyl radicals serve for development in wastewater decontamination processes, in air purification, and in the production of clean energy through the separation of water into $H_2$ and $O_2$. Furthermore, among the various advanced oxidation processes, heterogeneous photocatalysis is the most promising approach that has been significantly investigated in the last two decades due to its potential to completely remove organic compounds. Mechanism of photocatalysis using semiconductors is documented in the literature and a great deal of research has been carried out on the design and development of various photocatalysts. For instance, bismuth oxyhalides ($BiO_X$, X = F, Cl, Br, I) are a new class of two-dimensional materials that have attracted extensive interest owing to their tetragonal $PbFCl^-$ - type layered crystal structure with $[Bi_2O_2]^{2+}$ slabs interleaved by double slabs of halogen ions that produces an internal static electric field perpendicular to each layer [1-3]. The self-generated internal electric field produced in bismuth oxyhalides is favorable for the transport of electrons and photoinduced holes within the crystal, resulting in increased photocatalytic activity due to the greater separation of photogenerated charge carriers. There are various bismuth oxyhalides, such as BiOBr, which have attracted great attention due to its high stability, good electrical conductivity and relatively superior photocatalytic activity under visible light.

On the other hand, the formation of spatio-temporal patterns has been analyzed using various types of mathematical models from nonlinear chemistry [8]. From the biological point of view, the patterns formed by the numerical solutions of these models can be classified into two categories: chemical patterns and patterns of cell movement. In the category of chemical standards there are two types of models: gradient models and reaction-diffusion models [5, 6]. Reaction-diffusion models describe the chemical interactions that generate complex patterns in space and / or time, due to the presence of transport, synthesis and degradation terms that depend on all the chemical substances present in the analysis domain. Moreover, cell movement models analyze the formation of spatial patterns due to changes in cell density, by aggregation or repulsion between cells, or by response to specific chemical substances. In 1952 A. Turing was the first to observe and attribute to chemical interactions between substances the self-formation of patterns in nature [9] and studied the solutions of biological models described by reaction-diffusion equations. In them he found that there can be three types of instabilities: a) oscillatory in time and uniform in space, related to Hopf instabilities independent of space [4], b) stationary in time and periodic in space [5, 9], and c) oscillatory in space and time [8, 7]. Turing further demonstrated that a chemical reaction-diffusion system can evolve into heterogeneous spatial patterns from a uniform steady state in response to small perturbations. Accordingly, he established that diffusion can lead to chemical instability, thus inducing the formation of a spatial pattern where it did not previously exist. This type of instability, stationary in time, is better known as Turing instability.

In this research work, a reaction mechanism for ox-redox kinetics is proposed by interacting a hypothetical semiconductor with electromagnetic radiation in the ultraviolet. Subsequently, using the reaction mechanism obtained from nonlinear chemistry, a diffusion reaction system is deduced that presents Turing and Turing-Bogdanov-Takens instability. Using the numerical method of functional difference implemented in python and its libraries [10], a three-dimensional (3D) computational simulation is obtained from the numerical solution of the spatio-temporal kinetic of ox-redox carry out during the air remediation.

**1. Mathematical reaction-diffusion model for photocatalysis of bismute oxyhalides in air remediation**.

Photocatalysis process to the elimination of NOx-type gases and its photo-oxidation mechanism can be carried out through the reaction of the polluting gases with the hydroxyl and superoxide radicals generated during the activation of the semiconductor (SC), according to the series of chemical reactions represented by the sequence of basic reactions may be written as:

$$SC + h\upsilon \rightarrow SC\,(e^-_{BC}) + SC\,(h^+_{BV}) \quad (1)$$

$$SC\,(e^-_{BC}) + O_2 \rightarrow O_2^{\bullet -} + SC \quad (2)$$

$$SC\,(h^+_{BV}) + H_2O \rightarrow OH^\bullet + H^+ + SC \quad (3)$$

$$NO + OH^\bullet \rightarrow HNO_2 \quad (4)$$

$$HNO_2 + OH^\bullet \rightarrow NO_2 + H_2O \quad (5)$$

$$NO_2 + OH^\bullet \rightarrow NO_3^- + H^+ \quad (6)$$

$$NO + O_2^{\bullet -} \rightarrow NO_3^- \quad (7)$$

Performing the corresponding operations, from equations (1)-(3) and (7). Subsequently taking equations (4)-(6) two final equations are obtained

$$NO + 3OH^* \rightarrow NO_3^- + H_2O + H^* \quad (8)$$

$$O_2 + OH^- + NO \rightarrow OH^* + NO_3^- \quad (9)$$

Applying the law of mass action, we obtain:

$$V_1 = k_1[OH^*]^3[NO] \quad (10)$$

$$V_3 = k_2[NO][OH^-][O_2] \quad (11)$$

Assigning variables to interest and constants terms that can remain constant during the catalysis, substituting in the equations

$$x = NO,\ y = NO_3^-,\ z = OH^*,\ A = O_2.$$

Substituting the variables assigned to the proposed equations based on equations (10) and (11), if a compound is reactive, it will be subtracted in the equation, since it is consumed during the catalysis process, but if it is a product, it will be positive because it is generated in the reaction:

$$\frac{d[x]}{dt} = -k_1[z]^3[x] - k_2[x][OH^-][A] \quad (12)$$

$$\frac{d[y]}{dt} = k_1[z]^3[x] + k_2[x][OH^-][A] \quad (13)$$

$$\frac{d[z]}{dt} = -k_1[z]^3[x] + k_2[x][OH^-][A] \quad (14)$$

The hydroxyl radical (OH *) is an intermediate in the reaction for the formation of $NO_x$ compounds, therefore, this change tends to 0:

$$\frac{d[z]}{dt} = 0,$$

$$0 = -k_1[z]^3[x] + k_2[x][OH^-][A].$$

Solving $[z]^3$ from equation (14) we will obtain:

$$[z]^3 = \frac{k_2[x][OH^-][A]}{k_1[x]} \quad (15)$$

Substituting equation (15) into equations (12) and (13):

$$\frac{d[x]}{dt} = -2k_2[x][OH^-][A] \quad (16)$$

$$\frac{d[y]}{dt} = 2k_2[x][OH^-][A] \quad (17)$$

The analysis is simplified by converting these equations to a dimensionless form. The appropriate conversion factors are:

$$\frac{[x]k_1}{k_2[A]} = [X]\ \ donde\ k_1 = \frac{L^3}{s * mol^{-3}}, k_2 = \frac{L^2}{s * mol^{-2}}$$

Hydroxyl potential can be measured, so we establish a relationship by giving it a variable "L"

$$-log_{10}[OH^-] = pOH$$

$$[OH^-] = 10^{-pOH} = L$$

Introducing dimensionless parameters, we obtain a simpler form of the equations into (16) and (17):

$$\frac{d[X]}{dt} = -2xL\,, \quad (18)$$

$$\frac{d[Y]}{dt} = 2xL\,. \quad (19)$$

In order to perform a computational simulation, it is necessary to find the domain of the numerical solution of a system of nonlinear partial differential equations (NPDE). Applying the diffusivity term to the system of equations:

$$\frac{d[x]}{dt} = D_x\nabla^2[x] - 2x[L], \quad (20)$$

$$\frac{d[y]}{dt} = D_y\nabla^2[y] + 2x[L]. \quad (21)$$

This type of NPDE system is called a reaction-diffusion system (RDS). Thus, it is necessary to find this domain using a general analysis technique called *Linear Stability Analysis*. This technique of studying mathematical models to solve NPDE by making $\nabla^2 = 0$ using the finite difference numerical method.

$$F = -2x[L], \quad (22)$$

$$G = 2x[L]. \quad (23)$$

We must compute the fixed points defined as the roots of the nonlinear terms of an EDPN system by making $\frac{\partial[u]}{dx} = 0, \frac{\partial[u]}{dy} = 0, \frac{\partial[v]}{dx^2} = 0\,\frac{\partial[V]}{dy^2}$……,etc. Therefore, when substituting these conditions in the RDS we obtain: F (u (x, y, t), v (x, y, t), t) = 0, G (u (x, y, t), v (x, y, t), t) = 0. This new system must be solved by some method to calculate the roots (u0, v0), either to obtain the solutions exactly (u0, v0)

$$\frac{\partial[F]}{dx} = -2[L], \frac{\partial[F]}{dy} = 0, \frac{\partial[G]}{dx} = 2[L], \frac{\partial[G]}{dy} = 0 \quad (24)$$

Jacobian:

$$J(u,v) = \begin{pmatrix} \frac{\partial[F]}{dx} & \frac{\partial[F]}{dy} \\ \frac{\partial[G]}{dx} & \frac{\partial[G]}{dy} \end{pmatrix} \quad (25)$$

$$Tr[J(u,v)] = \frac{\partial[F]}{dx} + \frac{\partial[G]}{dy} = -2[L] \quad (26)$$

Determinant without the term of diffusion:

$$0 = \left| \lambda \begin{pmatrix} 1 & 0 \\ 0 & 1 \end{pmatrix} - \begin{pmatrix} \frac{\partial[F]}{dx} & \frac{\partial[F]}{dy} \\ \frac{\partial[G]}{dx} & \frac{\partial[G]}{dy} \end{pmatrix} \right| \quad (27)$$

Determinant with the term of diffusion:

$$0 = \left| \lambda \begin{pmatrix} 1 & 0 \\ 0 & 1 \end{pmatrix} - \begin{pmatrix} -2[L] & 0 \\ 2[\mathrm{L}] & 0 \end{pmatrix} - k^2 \begin{pmatrix} D_x & 0 \\ 0 & D_y \end{pmatrix} \right| \quad (28)$$

Solving:

$$\lambda^2 + \lambda\gamma + \omega = 0 \quad (29)$$

Where

$$\gamma = 2L + k^2(D_x + D_y) \;\; y \;\; \omega = 2Lk^2D_y + k^4D_xD_y$$

Deriving ω according to $k^4$and obtain $k^2$:

$$\omega' = 2LD_y + 2k^2D_xD_y \quad (30)$$

$$k^2 = -\frac{L}{D_x} \quad (31)$$

and defining:

$$D = \frac{D_y}{D_x} \quad (32)$$

Can be wrote $\gamma$ as:

$$\gamma = L(1-D), \qquad \omega = -2L^2\mathrm{D}. \quad (33)$$

Calculation of instabilities: the steady states of the RDS are those points where it reaches equilibrium and there is no dynamics (∂u / ∂ t = 0, ∂ v / ∂ t = 0), that is, at the fixed points (u0, v0). On the other hand, an unsteady state is where there is dynamics and the value of the eigenvalues determines the form of the RDS solutions and therefore the unsteady states:

$$\lambda\pm = \frac{1}{2}(\gamma) \pm \sqrt{(\gamma)^2 - 4(1)(\omega)}. \quad (34)$$

**2. Results analysis of linear stability and its computational simulation.**

**2.1. Spatio-temporal instabilities.**

To find the Turing instability (s) of our reaction system, which we will call the OH-$NO_x$ reaction model, we used the Gnuplot 5.2 graph, the parameters taken were "L" and "D", where L represents the concentration of hydroxyl radicals and D represents the concentration of nitrated compounds ($NO_x$), the range of values taken for L and D were 0 to 1 in both cases.

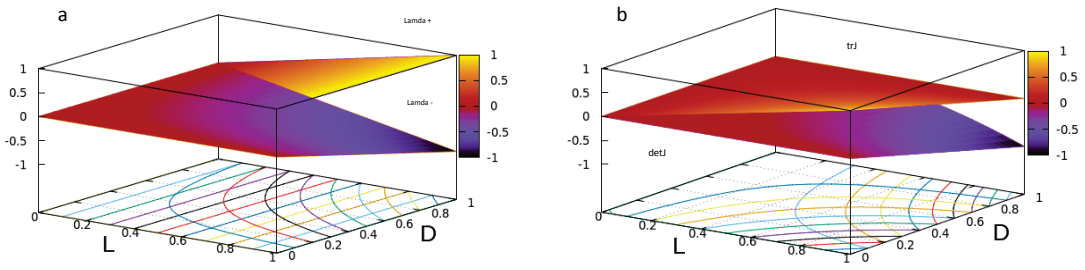


**Figure 1.** Turing instability graph (a) view of positive lamda (upper plane orange-yellow color) and negative lamda (violet color) lower plane, (b) view of the trJ and detJ, corresponding to a saddle point

**Table 1.** Parameters used for 3D simulations in Python

| pOH | pH | D | L | Figure 2 |
|---|---|---|---|---|
| 2 | 12 | 0.5 | $1x10^{-2}$ | C) |
| 7 | 7 | 0.15 | $1x10^{-7}$ | B) |
| 11 | 3 | 0.9 | $1x10^{-11}$ | A) |

Figure 2, according to the mathematical analysis of Turing instability that predicts the type and shape of the emerging patterns of the temporal solution of the reaction-diffusion equations for our system. The curvature of the contour lines in Figure 1 (a and b) colored lines that are shown along the planes at the bottom of both positive and negative images, as well as trA (trace) and detJ (determinant) that clearly denotes the type of instability called saddle point according to literature. This means that this state of stability is always unstable far from zero for the OH-NOx reaction model. In addition to it, is found a Turing-Bogdanob-Takens instability for $L << 1$ (see Fig. 1), it is: $1x10^{-2} >= L$.

**2.2. 3D Computer Simulation.**

Python 2.7.6 64-bit and Mayabi2 [11] were used to carry out the 3D modeling, runs were made for $L = 1x10^{-8}$ and $D = 0.5$ with the following parameters, grid size $128\ x128x128$, mesh size between node and node $dx = \pi / 4$, time step $dt = 0.01$, $Da = 5$ and $n = 100{,}000$ iterations and dimensionless time $t = n\ dt = 1000$.

The reaction-diffusion system was solved according to the parameters in the following table 1.

From table 1 the simulations were for three different pOH, each with different diffusion ratio factors D. Figure 3 (a) shows the behavior in the acid medium of the production of hydroxyl (left) and nitrated compounds (center) for the time 100 to 10,000 iterations which is the same as it is 50% for both, the diffusion can be observed in the red-orange zones themselves which are the regions of greatest concentration, the 3D simulation of the mixture (right) presents zones of high intensity in which the diffusion of both compounds distributed at random is carried out, the areas of king blue represent less diffusion.

a) OH NOx OH+NOx

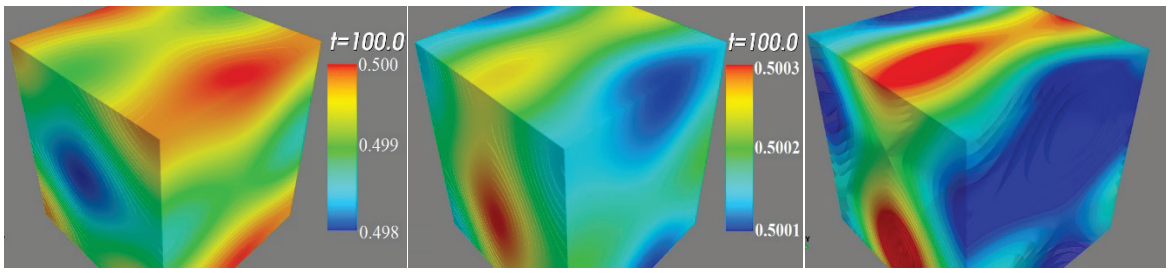


b) OH NOx OH+NOx

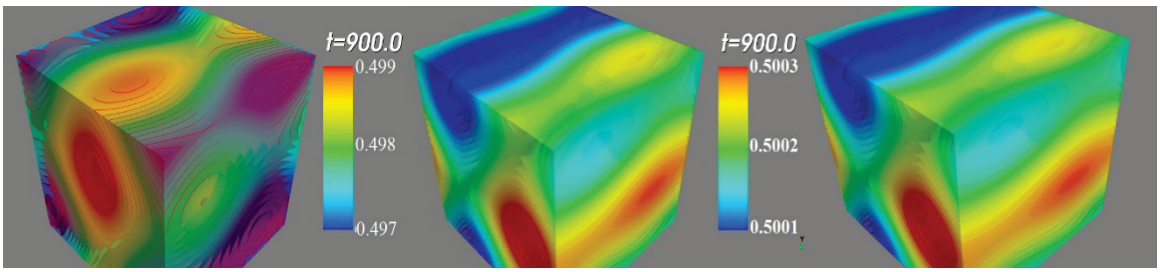


c) OH NOx OH+NOx

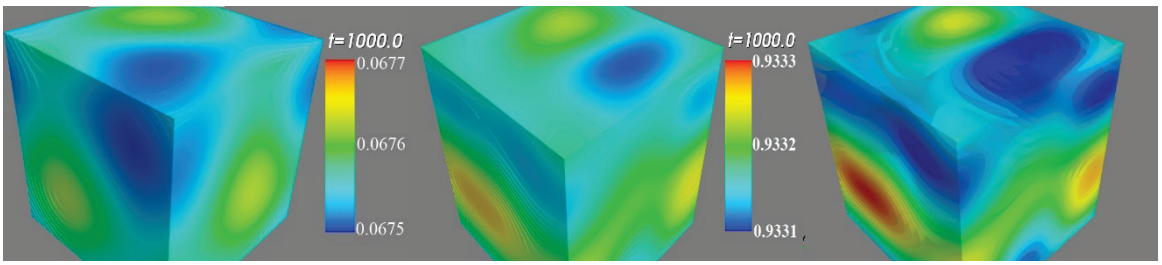


**Figure 2.** 3D simulations obtained by Python for hydroxyl radicals (left column), nitrated compounds (center columns) and mixture of both compounds (right column) for (a) time 100, (b) time 900, (c) time 1000. See Table 1 for known the values of control parameters D and L

By iterations recurring, is shows that the spatio-temporal diffusion dynamics of the production of nitrated $NO_x$ compounds and hydroxyl radicals under the influence of the photocatalyst of bismuth oxyhalides, is carried out in a controlled manner, the production is 50% just like an acid medium. 3D simulations show significant activity in the formation of hydroxyl (bottom left, left image) and nitrated $NO_x$ compounds (bottom left, central image), the diffusion in the mixture is concentrated in the same area as in the two previous images.

Finally, simulations were obtained for the basic medium at pOH 2 (pH 11), Figure 3 (c) represented for the dimensional time 1000 units (or 100,000 iterations), we can note that the diffusion and production process of both compounds is faster, we shows that the efficiency in a basic medium of nitrated compounds (NOx) (central image) effective, since, the production is 93% and only 6% of hydroxyl after the reaction is finished, the evolution over time describe an accelerated diffusion process for the formation of radicals and nitrated compounds.

**Conclusion.**

The mathematical model proposed for the description of reaction-diffusion due to Bismuth oxyhalide photocatalysts demonstrate that they are useful to exemplify the formation process of the compounds of interest. It can be seen how the hydroxyl potential (pOH) influences the reaction speed of the OH-NOx reaction model, since it can be seen how the diffusion is carried out with greater speed for more basic potentials and a slower behavior for high potentials. Conversely, the reaction rate is carried out for basic pH and is slower for acids, given the inverse relationship between pH and pOH. Furthermore, the existence of spatial instabilities such as diffusion-induced instability (Turing instability) and a type of critical instability (Turing-Bogdanov-Takens) due to small perturbations of the uniform steady state, and the relationship between these instabilities are shown, showing that Turing space is the number space where the parameters of a model meet the given formations and the formation of spatio-temporal patterns is possible.

***References:***

1. Montoya Maria. *Síntesis de oxihaluros de bismuto BiOX (x= Cl, Br, I) para su aplicación como fotocatalizadores en la purificación de aire por eliminación de gases tipo NOx*. Tesis de Doctorado, Universidad Autónoma de Nuevo León, 2017.

2. Shenoy Sridharan. *Bismuth oxybromide nanoplates embedded on activated charcoal as effective visible light driven photocatalyst*. 2020. DOI: 10.1016/j.cplett.2020.137435.

3. Bac1ha A.U.R., Nabi I., Fu Zh., Li K., Cheng H. *A comparative study of bismuth-based photocatalysts with titanium dioxide for perfluorooctanoic acid degradation*, 2019. DOI: 10.1016/j.cclet.2019.07.058.

4. Pouya Bastani. *Pattern Formation in the Gray-Scott Model.* Department of. Mathematics – Simon Fraser University, 2012.

5. Vanegas, Landinez, Garzón. Analysis of Turing instability in biological Models. *Dynamics, Universidad Nacional de Colombia*, 2018, vol. 76, no. 158, pp. 123-134.

6. Kishore Dutta. *Reaction-diffusion Dynamics and Biological Pattern Formation*. Department of Physics, Handique Girls' College, Guwahati, India, 2017.

7. Mazin W., Rasmussen K.E., Mosekilde E., Borckmans P., Dewel G. *Pattern formation in the bistable Gray-Scott model.* Physics Department, The Technical University of Denmark, DK- 2800 Lyngby, Denmark, Service de Chimie-Physique, Universitb Libre de Bruxelles, 1050 Brussels, Belgium, 1996.

8. Sagués F., Epstein I.R. Nonlinear chemical dynamics. *Dalton transactions*, 2003, no. 7, pp. 1201-1217.

9. Turing A.M. The chemical basis of morphogenesis. *Bulletin of mathematical biology*, 1990, vol. 52 (1-2), pp. 153-197.

10. Landau R.H., Pï M.J., Bordeianu C.C. *Computational physics: Problem solving with Python*. John Wiley & Sons, 2015.

11. Ramachandran P., Varoquaux G. Mayavi: 3D visualization of scientific data. *Computing in Science & Engineering*, 2011, vol. 13 (2), pp. 40-51.